CHANGES IN CLOUDINESS OVER TROPICAL LAND DURING THE LAST DECADES AND ITS LINK TO GLOBAL CLIMATE CHANGE

A Thesis
Presented to
The Academic Faculty

by

Paola Andrea Arias

In Partial Fulfillment
of the Requirements for the Degree
Master of Science in the
School of Earth and Atmospheric Sciences

Georgia Institute of Technology
December, 2008

CHANGES IN CLOUDINESS OVER TROPICAL LAND DURING THE LAST DECADES AND ITS LINK TO GLOBAL CLIMATE CHANGE

Approved by:

Dr. Rong Fu, Advisor
School of Earth and Atmospheric Sciences
Georgia Institute of Technology

Dr. Robert X. Black
School of Earth and Atmospheric Sciences
Georgia Institute of Technology

Dr. Robert Dickinson
School of Earth and Atmospheric Sciences
Georgia Institute of Technology

Date Approved: November 11, 2008

ACKNOWLEDGMENTS

Thanks to Rong Fu for her guidance and support, to Carlos Hoyos and Wenhong Li (Georgia Institute of Technology) for their helpful comments, Larry Oolman (University of Wyoming) for providing the radiosonde data, Aiguo Dai (National Center for Atmospheric Research, NCAR) for providing his global surface station data, and Felipe Quintero (Universitat Politecnica de Catalunya) for his help in processing the radiosonde data.

TABLE OF CONTENTS

Page

LIST OF TABLES

LIST OF FIGURES

SUMMARY

Tropical forests play a key role in determining the global carbon-climate feedback in the 21st century. Changes in rainforest growth and mortality rates, especially in the deep and least perturbed forest areas, have been consistently observed across global tropics in recent decades. Understanding the underlying causes of these changes, especially their links to the global climate change, is especially important in determining the future of the tropical rainforests in the 21st century. Previous studies have mostly focused on the potential influences from elevated atmospheric CO_2 and increasing surface temperature. Because the rainforests in wet tropical region are often light limited, we explore whether cloudiness have changed, and if so, whether it is consistent with what is expected from changes in forest growth rate.

CHAPTER 1

INTRODUCTION

Tropical forests contain as much as 40% of the carbon stored as terrestrial biomass and account for 30 to 50% of terrestrial productivity [Phillips et al., 1998].They act as an important sink for carbon dioxide (CO2), a gas emitted mainly from the burning of fossil fuels coal, oil and natural gas, but also by plants, animals, and human respiration, and the major driver of global climate change.

The Amazon and the Congo forests are the world's largest and second largest tropical forest respectively. The Amazon rainforest contributes around 10% to global terrestrial productivity and biomass [Malhi and Grace, 2000], 15% to global photosynthesis, and a quarter of the global biospecies. Its hydrological cycle is a key driver of global climate, and global climate is therefore sensitive to changes in this forest [Changnon and Bras, 2005]. The Congo basin forest covers 700,000 square miles in six countries, containing a quarter of the world's remaining tropical forest. This vast area hosts a wealth of biodiversity, including over 10,000 species of plants, 1,000 species of birds, and 400 species of mammals [USAID, http://www.usaid.gov/ locations/sub-saharan_africa/initiatives/cbfp.html]. Climate change threatens to substantially affect these tropical regions, which in turn is expected to alter global climate and increase the risk of biodiversity loss.

In situ ecological observations suggest a possible faster growth and mortality rates of the

tropical rainforest in the 1990s compared to those in 1980s [Malhi et al., 2002]. Several studies suggest that Amazon and other rainforests exhibit flushes of new leaf growth with increased photosynthesis in the dry season that closely coincide with seasonal peaks in solar irradiance [Saleska et al., 2003; Wright and van Schaik, 1994]. This increase in growth rate is more robust over the forests least disturbed by human activities (e.g. western Amazon) [Phillips et al., 1998] suggesting that direct impact of land use is unlikely to be the cause. Huete et al [2006] show basin-wide enhanced rainforest activity during the dry season and indicate that sunlight may have more influence than rainfall on rainforest productivity. Malhi and Wright [2004] studied trends in global climate of tropical rainforest regions during 1960-1998 and found that, as a whole, African tropical rainforests appear the most water stressed, and generally drier, at higher elevation, and cooler than those of other continents. An increase in favorable conditions for enhanced forest activity over the Amazon forest has been shown by Li et al. [2008], who found increased anomalous dry events over the southern basin during the recent years.

More evidences of change in Amazon forest activity has been provided by Phillips et al. [1998], who show a statistically significant increase in biomass over this forest since at least the late 1970s. Nemani et al. [2003] found that Net Primary Productivity (NPP) increased by more than 1% per year in this tropical region between 1982 and 1999 and speculated that increase in solar radiation, owing to declining cloud cover in these predominantly radiation-limited forests, is the most likely explanation for the increasing tropical NPP. Such decrease in cloudiness over South American continent has been observed by Warren et al [2007] using CDIAC station data during the period 1971-1996.

The findings mentioned above suggest that both climate and vegetation activity over tropical forests have changed over the recent decades. Because the rainforests in wet tropical regions are often light limited, we explore whether this change is consistent with what is expected from changes in forest growth rate. Understanding the underlying causes of these changes is important in determining the future of the tropical rainforests in the 21st century.

Both continental surface heating and sea surface temperatures (SSTs) in the tropical Atlantic and Pacific can affect the seasonality of Amazon rainfall [Fu et al., 2001], and for instance, its cloudiness. Li and Fu [2004] found that land surface latent heat flux is a more important source of atmospheric moisture than large-scale moisture transport during the dry and early transition season over the Amazon basin. Large-scale transport becomes more important as the onset approaches and during the wet season. Land surface water recycling during dry and transition seasons may amplify rainfall more during those periods than during the wet season. These and many other studies suggest the importance of moisture transport from adjacent oceans to the Amazon basin in determining seasonal and interannual variability of rainfall, and for instance also cloudiness variability, over this tropical forest.

The main goal of this thesis is to explore the existence of changes in cloudiness over Amazon and Congo forests during the last decades and to look for possible links with changes in land surface and moisture transport from adjacent oceans. Trends in total and convective cloud fraction and shortwave downwelling (SW) radiation over these tropical forests are analyzed. Surface in situ data is used to identify trends in surface temperature, specific humidity, and relative humidity over these regions. Radiosonde data is used to analyze changes in temperature, specific humidity, and buoyancy vertical profiles over southern Amazon during last

decades.

To connect changes in cloudiness over Amazon basin with changes in moisture transport from adjacent oceans, trends in vertical velocity, vertically integrated moisture divergence, OLR, and SSTs are analyzed. Seasonal correlations between detrended SST and domain average omega at 700 and high-level clouds over both northern and Amazon are calculated in order to identify associations between those variables at interannual timescales. Seasonal correlations between detrended high cloud cover and warm pool areas are also estimated.

Finally, in order to address the question if whether changes in cloudiness and moisture transport over Atlantic Ocean and Amazon basin are linked to anthropogenic effects, seasonal trends in omega at 700 hPa from NCAR-CCSM3 20c3m experiment are calculated.

This thesis is distributed as follows. Chapter 2 describes the databases used in this study. Chapter 3 presents a brief overview of rainfall climatology over Amazon and Congo basins. Trends in ISCCP and land surface changes during the period 1984-2002 are discussed in Chapters 4 and 5, respectively. A brief revision about impacts of deforestation and land use changes in rainfall over Amazon forests is presented in Chapter 6. Although it is not the main goal of this study, trends in GIMMS NDVI are calculated to explore if land use changes have been observed during the last decades in the forests studied here. Chapter 7 discusses the main results about changes in moisture transport over ocean and land and its impact on changes of cloudiness over Amazon basin. Finally, conclusions obtained from this study are shown in Chapter 8.

CHAPTER 2

DATA AND METHODOLOGY

We use the monthly data from the International Satellite Cloud Climatology Project (ISCCP D2) database for clouds and shortwave (SW) downwelling radiation during 1984-2004 for a 2.5-degree resolution [Rossow and Schiffer, 1999], available at ISCCP website [http://isccp.giss.nasa.gov/index.html].

Monthly precipitation is obtained from the Global Precipitation Climatology Project (GPCP) on a 2.5-degree resolution for the period 1979-2006. GPCP data is provided by the NOAA/OAR/ESRL PSD and can be obtain from their Web site at http://www.cdc.noaa.gov/ [Adler et al., 2003]. Surface temperature, relative humidity, and specific humidity records correspond to in situ data interpolated in a 5 x 4-degree grid for the period 1976-2005 and are provided and described by Dai [2006].

Vertically integrated moisture divergence is calculated using monthly 2.5-degree resolution data for horizontal wind field and specific humidity at different pressure levels from the European Centre for Medium-Range Weather Forecasts (ECMWF) ERA-40 reanalysis [Simmons and Gibson, 2000]. The vertical integration is done between 1000 hPa and 600 hPa levels. ERA-40 vertical velocity (omega) fields at different pressure levels are also used.

ERA-40 horizontal wind field and specific humidity are also used to calculate vertically integrated moisture flux balance (VIMFB) over each of the tropical rainforests analyzed in

this study. Similarly to the moisture divergence, flux balance is integrated over the mid-lower troposphere, between 1000 hPa and 600 hPa levels. VIMFB is calculated by integrating the moisture flux over the box defined by the limits of the forest in consideration, as shown by Li and Fu [2004].

Radiosonde data are provided by University of Wyoming and correspond to daily measurements of temperature and specific humidity at 1200Z during 1980-2006 over five stations located in the Amazon basin [http://www.weather.uwyo.edu/ upperair/sounding.html]. Buoyancy is calculated between 1000 and 250 hPa with an interval of 5 hPa and is given by the difference between virtual temperatures of the air parcel and the ambient air. Virtual temperatures are obtained following Zhang [2002].

The Normalized Difference Vegetation Index (NDVI) dataset considered in this study is produced by the Global Inventory Modelling and Mapping Studies (GIMMS). This dataset corresponds to a 22-year (1981-2002) satellite record of monthly changes in terrestrial vegetation on a $\frac{1}{4}$-degree grid and it is available at the International Satellite Land-Surface

Climatology Project, Initiative II data archive [http://islscp2.sesda.com/ISLSCP2 _1/data/ vegetation/gimms_ndvi_monthly_xdeg/].

Finally, we use monthly NOAA interpolated Outgoing Longwave Radiation (OLR) on a 2.5-degree resolution [Liebmann and Smith, 1996]. Extended Reconstructed SST (ERSST) from NOAA-NCDC during the period 1854-present on a monthly 2-degree grid [Reynolds, 1988] is also used.

All the trends are analyzed for the period 1984-2002 and tested using a Mann-Kendall

test with an estimator proposed by Sen [1968] at a 95% confidence level. Linear correlations are also tested using a t-test at a 95% confidence level.

CHAPTER 3

BRIEF OVERVIEW OF RAINFALL CLIMATOLOGY OVER AMAZON AND CONGO BASINS

3.1 Rainfall climatology over Amazon basin

Figure 3.1 shows the observed climatological monthly mean precipitation over South America for October, January, April, and July in the period 1979-1993 (from Wang and Fu [2002]). The onset of the wet season starts in the equatorial western Amazon during SON, spreading quickly to the east and the southeast, and followed by a wet season with abundant rainfall across the Amazon basin during DJF. For MAM, regions of large precipitation reduce in size and migrate slowly toward the equator, indicating the end of the Amazon rainy season. The dry season occurs during JJA and extreme precipitation events are mainly confined north of the equator. This evolution indicates that the annual cycle over the Amazon basin involves a significant meridional migration of precipitation between south and north of the equator.

This meridional migration is the reason for a wet season peaking during DJF over the southern Amazon and the delayed peak during MAM over the northern region [Marengo, 2005]. SON constitutes the transition from dry to wet conditions over the southern Amazon and the driest season over the northern region. The seasonal changes in precipitation over the northern Amazon are thus larger than those over the southern Amazon.

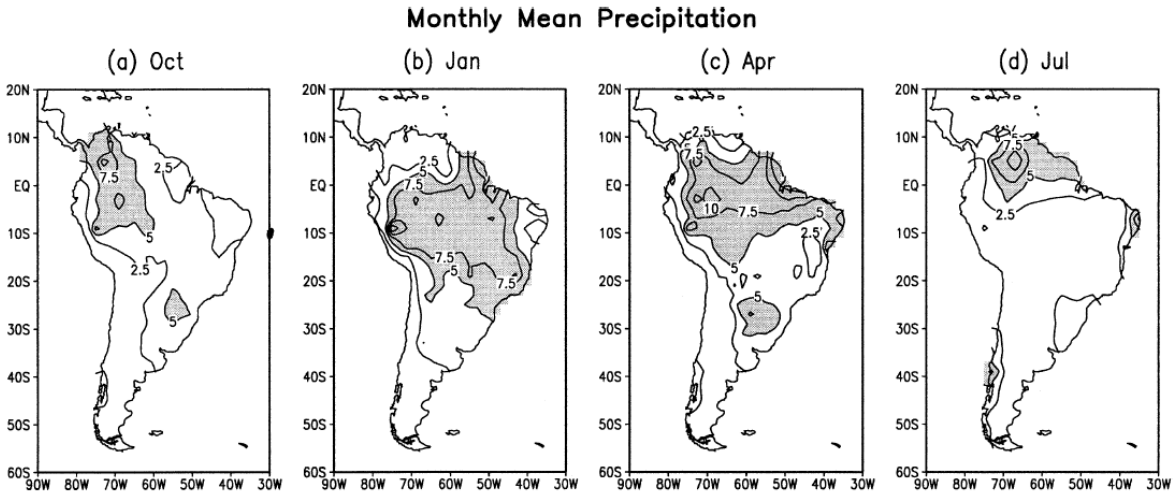

Figure 3.1: Observed climatological monthly mean precipitation over South America for October, January, April, and July in the period 1979-1993. Rainfall greater than 5 mm/day are shaded. Taken from Wang and Fu [2002].

Because of the described differences in climatological annual cycle over the northern and southern regions of the Amazon forest, the analyses shown in this study are performed separately for both regions. The northern Amazon was considered between 5°N and 5°S, while the southern region was selected between 5°S and 15°S. Both regions are located between 70°W and 50°W (Figure 3.2). The average rainfall annual cycle over both the northern and southern Amazon calculated using GPCP data for the period 1979-2006 is shown in Figure 3.3.

3.2 Rainfall climatology over the Congo basin

Figure 3.2 shows the Congo forest region (10°E-40°E and 5°N-10°S) considered in this study. The annual cycle of precipitation over this region for the period 1979-2006 (Figure 3.3) has two wet seasons, the first one peaking during MAM and the second one during

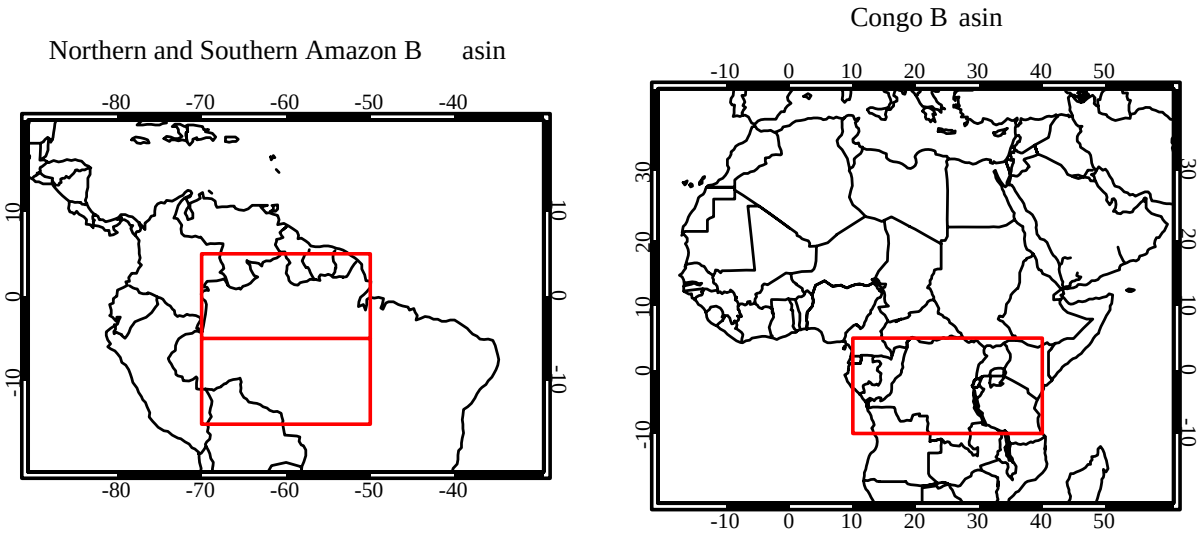

Figure 3.2: Location of the tropical forests considered in this study.

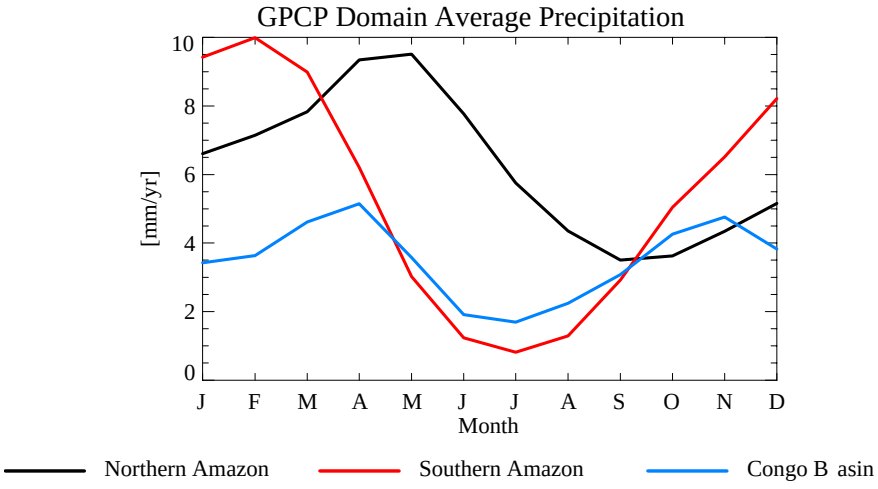

Figure 3.3: GPCP average annual cycle of precipitation over the tropical forests considered in this study (Figure 3.2). Averages are calculated during the period 1979-2006.

SON, both of them with similar amplitudes. There is a stronger dry season during JJA and a moderate one during DJF. This description coincides with results found by Balas et al. [2006].

Balas et al. [2006] studied SST influence on precipitation variability over west central Africa and found that the influence of Pacific, Atlantic, and Indian oceans is seasonally dependent. The Pacific is important mainly in MAM while the prime influence in JJA comes from the Atlantic. The impact of SST anomalies is seasonally dependent, enhancing rainfall in one season, but reducing it in the following season. These SST/rainfall associations over equatorial Africa are generally not symmetric in the sense that the factors producing wet conditions are not the reverse of those producing dry conditions.

CHAPTER 4

TRENDS IN ISCCP CLOUDS

Figure 4.1 shows the seasonal trend in ISCCP total cloud cover during 1984-2002 over the Tropical Americas and Africa. Trends shown are significant at 95% according to the Mann-Kendall test. Results indicate a decrease in total cloudiness over the Amazon basin during all the seasons consistent with an increase in SW downwelling radiation (not shown here). The largest changes are observed during SON and MAM over northern and southern Amazon, respectively. Decreasing trends in total cloudiness over South American continent has been shown by Warren et al [2007] using CDIAC station data during the period 1971-1996. Reductions in total cloud cover over the Congo region are clear during MAM and SON, which correspond to the wet seasons in this forest (see Figure 3).

Recent studies have highlighted the sensitivity of ISCCP cloudiness to changes in azimuth satellite angle caused by satellite reposition [Campbell, 2004; Norris, 2005a; Evan et al., 2007]. Norris [2005a] found that an increase in the number of geostationary satellites over time has produced a tendency towards lower viewing angles at many locations, thus generating an apparent decline in ISCCP planetary albedo and cloud cover. However, not all the types of clouds are equally biased by changes in azimuth satellite angle. ISCCP clouds are detected using the called "threshold method". Since clouds are almost always brighter and colder than the surface, the darkest and warmest pixels are identified as clear sky and

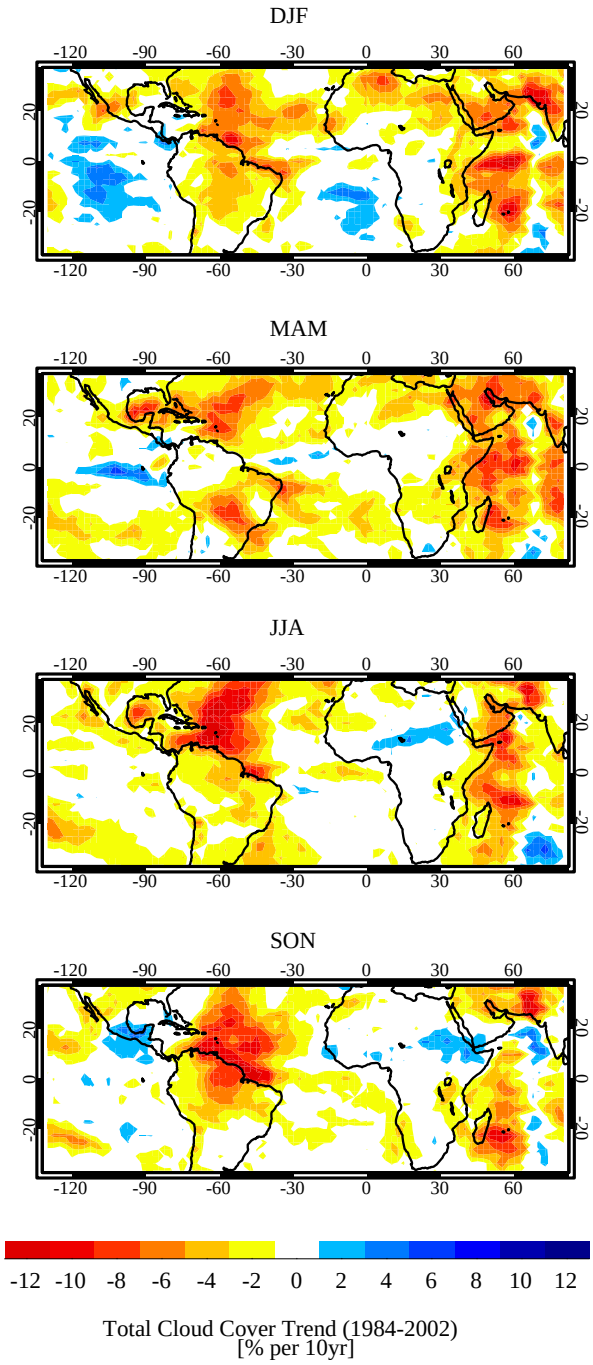

Figure 4.1: Seasonal trend in total cloud cover from ISCCP during 1984-2002 over the Tropical Americas and Africa. Values over the oceans are masked. Trends are significant at 95% according to the Mann-Kendall test with Sen's statistic [Sen, 1968].

pixels brighter and colder beyond a certain threshold are identified as cloudy [Norris, 2000a]. This fact explains why low-level clouds are more sensitive to small changes in temperature due to shift of azimuth angle than middle and high-level clouds. Figure 5 shows seasonal trends for low, middle, and high-level clouds from ISCCP during 1984-2002. Results indicate that low-level clouds over both Amazon and Congo basins do not have any significant trend. This suggests that the decreasing trend in total cloud cover over Amazon and Congo forests shown in Figure 4.1 is not biased by satellite azimuth angle change since it is mainly contributed by high and middle-level clouds over these tropical forests. However, low-level clouds over oceans do show significant decreasing trends (not shown here), indicating that trends in total clouds are biased by satellite azimuth angle change. Figure 4.2 suggests that ISCCP clouds over tropical oceans are not reliable.

Decreasing trends are also observed in high-level (precipitation) clouds over the most of the Amazon basin. This reduction agrees with the decrease in precipitation and drier conditions observed over this forest during the last decades [Marengo, 2004]. However, it is remarkable the local increase in high-level clouds observed over the northeastern Amazon during MAM (wet season; Figure 4.3). Total cloud cover does not exhibit any significant change over this region during MAM, since the increase in high-level clouds is compensated by the decrease in middle clouds. On the other hand, the decrease in total cloudiness observed over Congo basin during MAM is due to a decreasing middle-level cloud cover, while the decrease during SON is caused by a reduction in high-level clouds, as it is shown in Figure 4.2.

Figure 4.4 shows the annual cycle of total, low, middle, and high-level clouds averaged

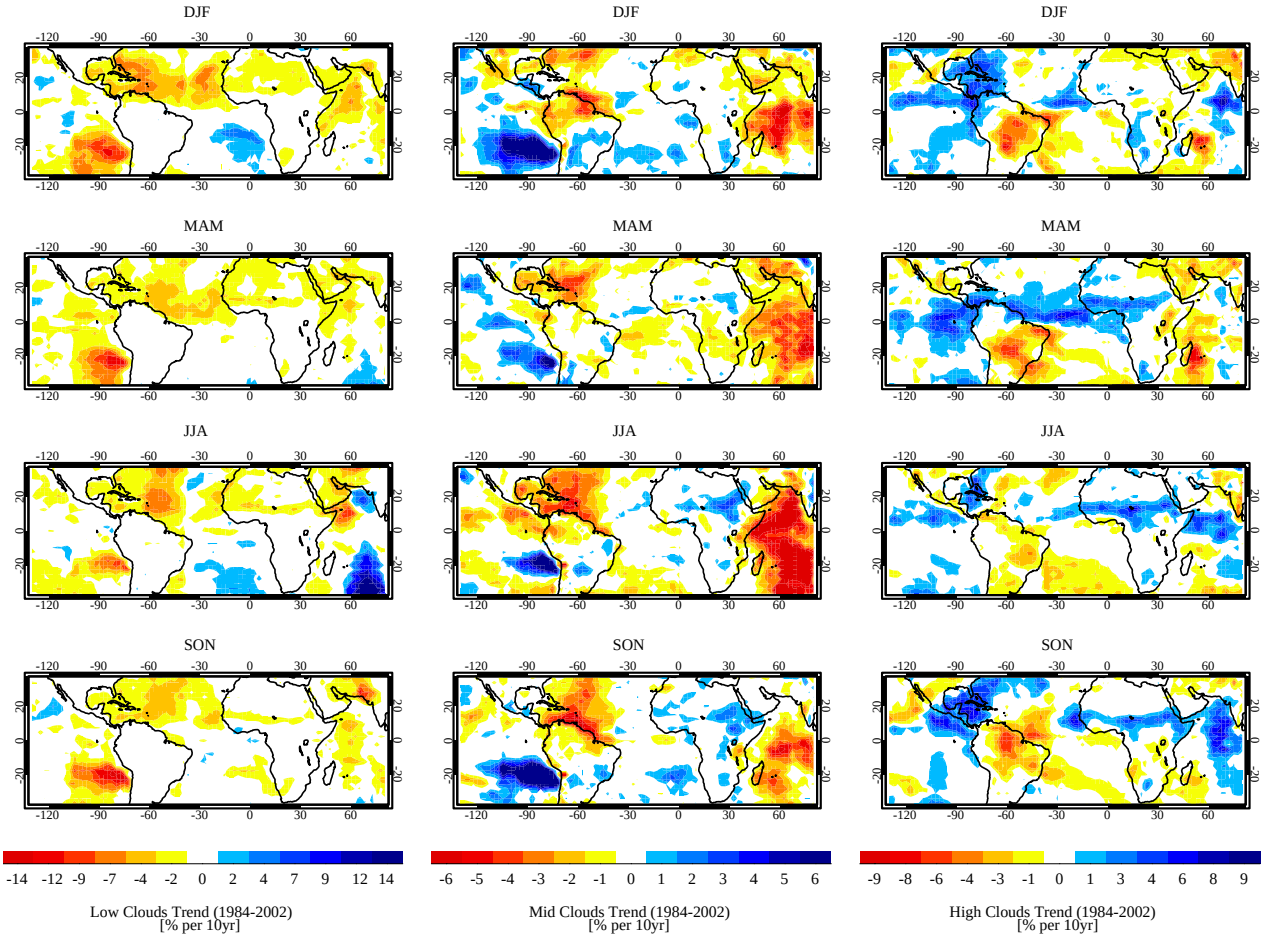

Figure 4.2: Same as Figure 4.1 but for ISCCP low, middle, and high-level clouds.

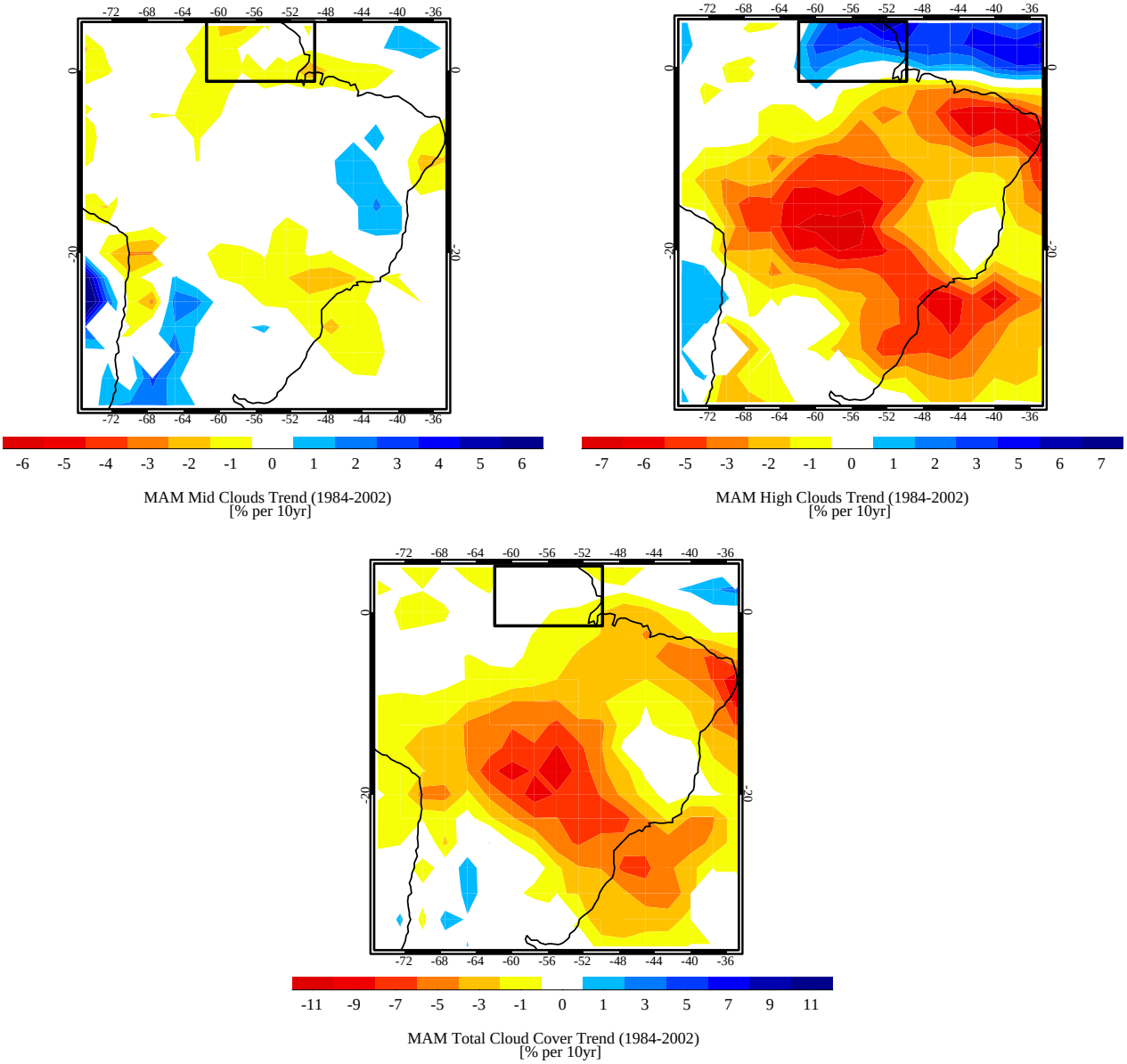

Figure 4.3: MAM trends for ISCCP middle-level, high-level and total clouds over the Amazon basin during 1984-2002. Boxes correspond to the region where convective clouds increase (northeastern Amazon). Trends are significant at 95% according to the Mann-Kendall test with Sen's statistic [Sen, 1968].

over the forests in which this study is focused. Annual cycles for total and high clouds agree with the precipitation annual cycles over these regions presented in Figure 3. This also indicates consistency and reliability in ISCCP data over these specific regions since high-level clouds (cirrus, cirrostratus, and deep convective clouds) are the responsible for more than 80% of precipitation over the Amazon [Greco et al., 1990]. Figure 7 also evidences that total cloud cover over Amazon and Congo forests is mainly constituted by high-level clouds. Lower and middle cloud types do not show a strong variability throughout the year.

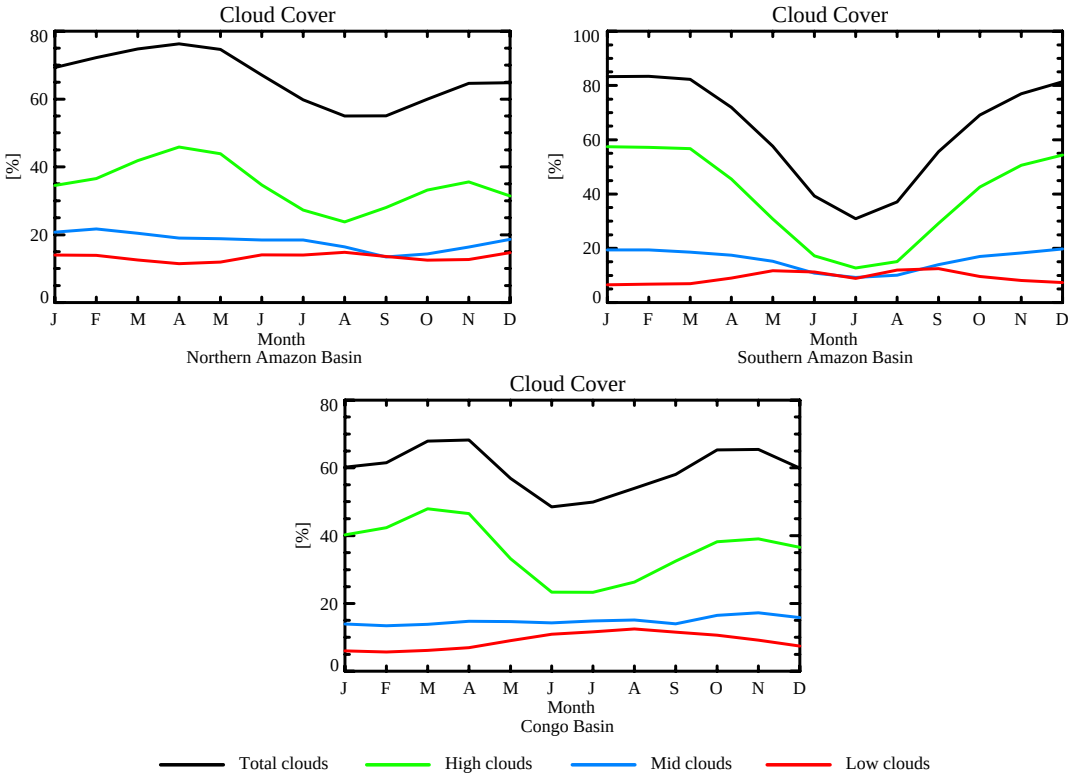

Figure 4.4: Average annual cycle for ISCCP total, low, middle, and high-level clouds over northern and southern Amazon and Congo basins. Averages are calculated for the period 1984-2004.

CHAPTER 5

CHANGES IN AND THERMODYNAMIC CONDITIONS OVER AMAZON AND CONGO FORESTS

In order to link such observed changes in cloudiness to changes in surface conditions over both the Amazon and Congo forests, seasonal trends for surface temperature, specific humidity, and relative humidity using the datasets described by Dai [2006] are analyzed. Table 5.1 shows the seasonal trends for these variables averaged over the domains shown in Figure 3.2. Results indicate an increase in surface temperature over Amazon and Congo basins during all the seasons, in agreement with findings by Malhi and Wright [2004], who suggest that since the mid-1970s all tropical rainforest regions have experienced a strong warming, in synchrony with a global rise in temperature that has been attributed to the anthropogenic greenhouse effect.

Surface relative humidity decreases for JJA-SON (dry season) over the northern Amazon and SON (transition season) over the southern Amazon. This result suggests stronger dry season over the Amazon forest during the last two decades, in agreement with Li et al. [2008], who have shown increase in anomalous dry events over the southern Amazon basin (5°S-15°S) during recent years. It is important to mention that the trends in humidity observed over Amazon forest would lead to a decadal-scale change that is comparable to humidity reductions from wet to dry season. Dai [2006] shows that the decreasing trend in

Table 5.1: Seasonal trends for surface temperature, relative humidity, and specific humidity averaged over the regions shown in Figure 2. Values represent the total change in each variable during 1984-2002.

	DJF	MAM	JJA	SON
	Northern Amazon			
T (°C)	0.2	0.1	0.6	0.7
RH (%)	0.8	2.2	-1.9	-4.1
	Southern Amazon			
T (°C)	0.2	0.5	0.8	0.6
RH (%)	1.5	1.4	1.4	-1.1
	Congo Basin			
T (°C)	0.7	1.1	0.7	0.4
RH (%)	-0.5	-3.9	-3.3	-4.1
q (g/kg)	-0.2	-0.4	-0.2	-0.5

relative humidity is correlated with a trend of increasing surface temperature. Results for the Congo basin indicate a decreasing trend in both relative and specific humidity at surface during all the seasons, which is consistent with the dryer and warmer conditions observed during the last decades over this forest [Malhi and Wright, 2004].

Vertically integrated moisture flux balance (VIMFB) was calculated over each one of the forests considered in this study (Figure 2). VIMFB trends (not shown here) indicate statistically significant decreasing trends in moisture flux convergence during JJA and SON over northern Amazon, MAM, JJA, and SON over southern Amazon, and MAM and JJA over the Congo forest. This suggests drier conditions in the mid-lower troposphere over both the Amazon and Congo forests, especially during the dry and transition seasons over the Amazon basin where these decreasing trends are consistent with a decreasing high-level cloud cover (Figure 5) and surface humidity (Table 1) observed during these seasons. The meridional component of the vertically integrated moisture flux balance exhibits a statisti-

cally significant increasing trend during MAM over the northern Amazon (not shown here), which is consistent with the increase in high-level clouds over the region observed for this season (Figure 4.3).

Both surface data from stations and vertical data from reanalysis indicate drier conditions over the tropical rainforests considered here. To compare these results with those obtained from radiosondes, station data over the southern Amazon during 1980-2006 at 1200Z are used. Since the most reliable records from radiosonde data over this region correspond to Vilhena, located in southern Amazon at 60.10°W-12.70°S, only results for this station are shown. Buoyancy profiles were calculated from temperature and specific humidity given by the radiosondes at each level pressure between 1000 and 250 hPa with an interval of 5 hPa. Figure 5.1 shows the differential seasonal vertical profiles for temperature, specific humidity, and buoyancy, obtained as the difference between the profiles averaged during 1991-2002 and those averaged during 1984-1990. Results show a decrease in lower troposphere specific humidity, while values above 4 km height remain nearly the same during the last decades, indicating stronger dry conditions near surface.

Vertical profiles show a cooling over most of the troposphere, except during the dry season (JJA) when warmer conditions near surface are observed. This surface warming produces the increase in buoyancy over the lower troposphere observed during this season (Figure 5.1). With exception of this increase in surface buoyancy during the dry season, vertical profiles indicate decreasing buoyancy during the last decade. Vertically integrated buoyancy differences show reductions in all the seasons during the last decade, which is associated with a more stable troposphere and inhibition of convection.

ISCCP data averaged over the area where this station is located show reductions in both total and convective cloudiness during 1984-2002. Calculations of Convective Available Potential Energy (CAPE) obtained from the radiosonde data and vertically integrated moisture flux from ERA-40 data over Vilhena station (not shown here) indicate decreasing trends during the period of analysis. Level of free convection (LFC) over this station (not shown here) exhibits an elevated height during the last decade. Results from Vilhena radiosonde data are in agreement with the decreasing trends in convective clouds and moisture flux observed over the southern Amazon forest since 1984 found in this study.

Saleska et al. [2003], Wright and van Schaik [1994], among others, found that Amazon forests exhibit flushes of new leaf growth with increased photosynthesis during the dry season that closely coincide with seasonal peaks in solar irradiance. In addition, Huete et al [2006] showed a basin-wide enhanced rainforest activity during dry season, indicating that sunlight may have more influence than rainfall on productivity over this tropical forest. This conclusion is consistent with findings by Nemani et al. [2003], who indicate that Amazon forests are predominantly radiation-limited. As this study has shown, ISCCP data suggests an increase in surface SW downwelling radiation over Amazon basin during its dry and transition seasons (JJA and SON), in agreement with the enhanced productivity observed during these seasons in this tropical forest. This study also suggests an increase in SW downwelling radiation during the wet seasons over the Congo basin that is associated with decreasing total cloudiness. This increase in surface solar radiation could in principle contribute to the increasing growth rate in African forests observed by Malhi et al., [2002].

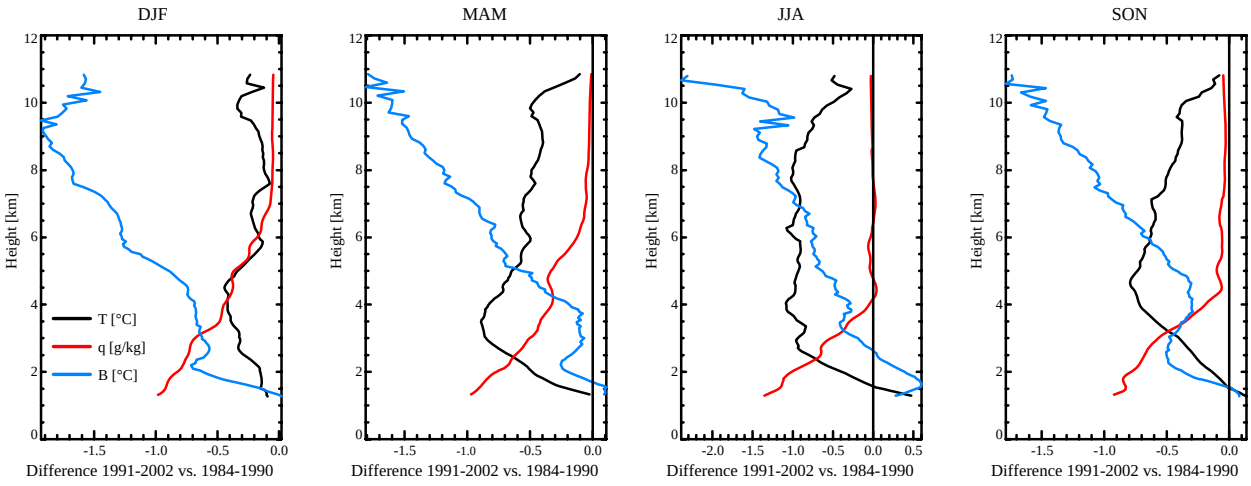

Figure 5.1: Seasonal difference profiles in temperature, specific humidity, and buoyancy calculated from radiosonde data for Vilhena (southern Amazon basin) at 1200Z. Differences are calculated between 1991-2002 and 1984-1990 periods.

CHAPTER 6

LAND USE AND VEGETATION CHANGES OVER TROPICAL FORESTS

Current climate and vegetation coexist in a dynamic equilibrium that could be altered by large perturbations in any of the two components. Until the early 1990's, deforestation was the dominant source of increased CO2 in the atmosphere. Since that time, the burning of fossil fuels has surpassed deforestation, but deforestation alone is estimated to be responsible for 35% of the greenhouse effect. If the wood is burned or decays, carbon stored in the wood of the trees is released into the atmosphere as CO2 and carbon absorption ceases.

Over tropical South America, deforestation is concentrated in the southern and eastern fringes of the Brazilian Amazon and along the major transportation lines in the interior [Chu et al., 1994]. The complex patterns of current levels of deforestation enhance shallow cumulus cloud cover over deforested areas [Changnon et al., 2004]. Rainfall accumulations have decreased significantly at the end of the wet season, and have increased at the end of the dry season [Chagnon and Bras, 2005]. Fu and Li [2004] suggested that increased land use change could delay the wet season onset and prolong the dry season by as much as several months given a similar large-scale atmospheric circulation pattern to today's.

Although precipitation trends in the Amazon are not clear, and multidecadal rainfall

variations have shown opposite tendencies in the northern and southern portions of the basin [Marengo et al., 2000], recent studies have clarified the link between deforestation and precipitation in the Amazon. Chagnon and Bras [2005] have found that current deforestation causes a dramatic change in climatological rainfall occurrence patterns, producing significantly more rainfall occurrence over deforested areas. Negri et al. [2004] found that in the dry season, when the effects of the surface cloudiness are not overwhelmed by large-scale weather disturbances, shallow cumulus cloudiness, deep convective cloudiness, and rainfall occurrence are larger over the deforested and nonforested (savanna) regions than over areas of dense forest.

Fire-assisted conversion of forests to agriculture and pastures promotes drought by decreasing water vapor flux (evapotranspiration) to the atmosphere, further inhibiting rainfall [Nepstad et al., 2001]. On the other hand, biomass burning provides a strong contribution of aerosols into the atmosphere, and for instance, affects precipitation, cloud properties, and radiative balance. Lin et al. [2006] show that elevated aerosol optical depth over the Amazon during the dry, biomass burning season (August-October) is associated with decreased cloud top temperature, suggesting higher cloud tops and increased rainfall. However, precipitation in southern Amazon (biomass burning centers) does not have positive trend [Marengo, 2004; Malhi and Wright, 2004]. In northeastern Amazon, precipitation appears to increase, but biomass burning in that region is minimal. Zhang et al. [2008] use regional model simulations to suggest that the smoke aerosols may decrease clouds within smoke area, but increase cloudiness in the northwestern Amazon.

The effects of deforestation and selective logging may change the local microclimate and

fire regimes, resulting in widespread collateral damage to the forest. Forest clearance and selective logging increase fire occurrence by providing abundant fuel loads and forest edges that are more vulnerable to desiccation during prolonged periods of dry weather [Foley et al., 2007]. Under natural conditions, fires are a rare occurrence in Amazon forests, for this reason many tree species are highly vulnerable under even low-intensity fires.

As it has been briefly described, land use and vegetation changes may exert important effects on cloudiness and precipitation not only over the Amazon, but also over the Congo forests. Although the goal of this study is not focused on the determination of such impacts, trends for Normalized Difference Vegetation Index (NDVI) are calculated in order to observe possible land use changes over the tropical forests studied here.

NDVI is an index related to the fraction of photosynthetically active radiation, hence serves as a measurement of greenness and vigor of vegetation. Figure 6.1 presents JJA and SON multiannual averages and trends for NDVI from Global Inventory Modelling and Mapping Studies (GIMMS) based on 1984-2002 period over tropical America and Africa. Since NDVI is a quantity calculated from reflectances measured in the visible and near infrared channels from satellite-based remote sensing, it is biased by cloudy conditions. Because of this bias, trends during DJF and MAM are not shown, since they correspond to the wet seasons over southern and northern Amazon, respectively.

Left panel of Figure 6.1 shows the climatological seasonal mean NDVI during JJA and SON. The largest NDVI values are observed during JJA over the southern Amazon. This is consistent with previous results by Saleska et al. [2003], Wright and van Schaik [1994],

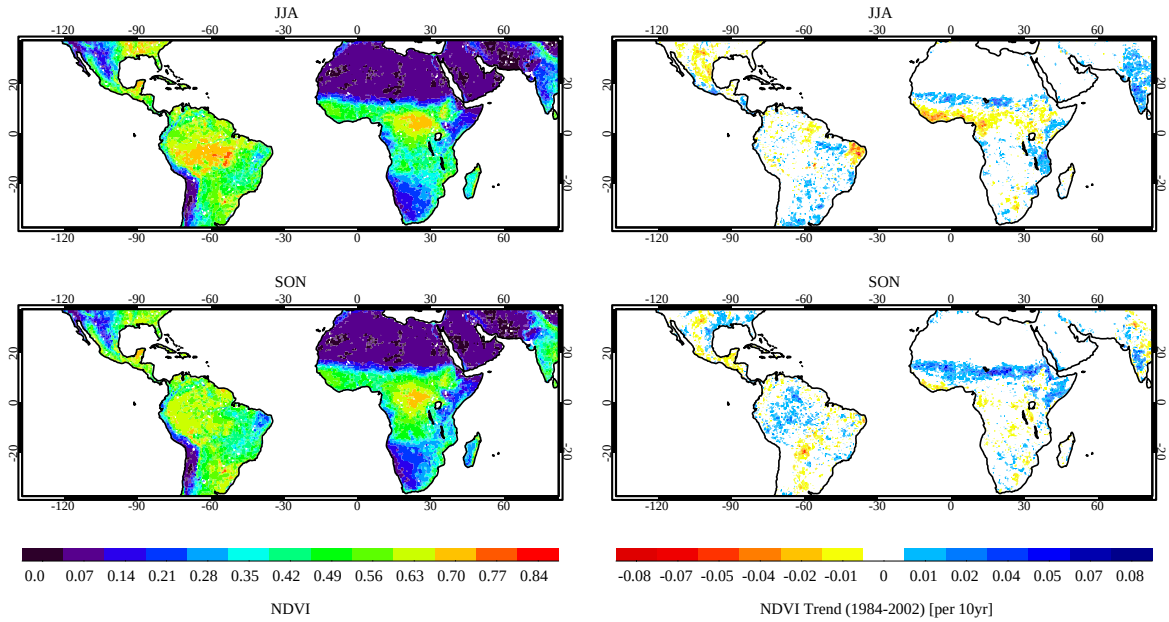

Figure 6.1: Seasonal averages (left panel) and trends (right panel) for NDVI from Global Inventory Modelling and Mapping Studies (GIMMS) over tropical America and Africa during JJA and SON. Both seasonal averages and trends are calculated for the period 1984-2002. Trends are significant at 95% according to the Mann-Kendall test with Sen's statistic [Sen, 1968].

and Huete et al [2006], suggesting an increased photosynthesis and greening over this forest during the dry season.

Seasonal trends are shown in the right panel of Figure 6.1. Statistically significant decreasing trends in NDVI (related to land use change) are observed over central-western Brazil during JJA and southern Brazil during SON. However, these regions are located outside the domain considered in this study (shown in Figure 2). Greening trends over the most of the Amazon basin are observed in both seasons, although whether such a greening is an artifact of cloud changes needs to be further investigated.

NDVI trends over Tropical Africa exhibit a continuous band of increasing trend over the Sahel region, consistent with the greening trend observed over this region since 1983 and discussed by different authors [Olsson et al., 2005]. Congo basin does not show significant trends in NDVI during the dry season (JJA), although there are significant decreasing trends during SON. However, since SON is the second rainy season over this forest, these trends could be an artifact produced by an increase in cloud cover during this season. Even though NDVI trends suggest that severe land use changes do not take place over the domains analyzed in this study, the effect of vegetation and land use changes in cloudiness over these tropical forests needs to be addressed.

CHAPTER 7

CHANGES IN MOISTURE TRANSPORT FROM ADJACENT OCEANS TO AMAZON BASIN IN PAST DECADES AND ITS EFFECTS ON CLOUDINESS

Both continental surface heating and sea surface temperatures (SSTs) in the tropical Atlantic and Pacific can affect the seasonality of Amazon rainfall [Fu et al., 2001], and for instance, its cloudiness. The relative contributions from ocean and land to Amazon precipitation vary across the different regions of this forest. Pacific SSTs influence eastern Amazon by causing dry conditions during El Niño events; however, its effects over western equatorial Amazon have not been clearly identified. Although effects of ENSO over Amazon precipitation are well established, the underlying mechanisms for these effects have not been completely understood.

Li and Fu [2004] found that land surface latent heat flux is a more important source of atmospheric moisture than large-scale moisture transport during the dry and early transition season over the Amazon basin. Large-scale transport becomes more important as the onset approaches and during the wet season. Land surface water recycling during dry and transition seasons may amplify rainfall more during those periods than during the wet season.

Whether the local land surface fluxes or remote influences from adjacent oceans control the rainfall and circulation of the wet season over Amazon forests is a continuous debate. Some authors argue that the land surface fluxes are the main contributors in the wet season and control its circulation pattern over the region [Rao and Erdogan, 1989]. On the other hand, other studies suggest that the SSTs in the tropical Atlantic and Pacific oceans strongly control the precipitation over the Amazon forests through the direct thermal circulation of the Atlantic ITCZ, as well as by Rossby waves propagating from the extratropical South Pacific to the subtropical South America [Fu et al., 2001].

Li and Fu [2006] suggest that more frequent and stronger cold air intrusions of extratropical cold air into South America trigger the early onsets of wet seasons given suitable large-scale thermodynamic conditions. Their analyses suggest that the abnormally strong jet stream tend to confine cold air to the subtropical region, therefore delaying the increase of precipitation during the transition from dry to wet season over the Amazon basin.

Recent studies by Hoyos and Webster [2007] have shown a general expansion of global thermodynamical warm pool. Especially, they have identified an eastward expansion of the Western Pacific warm pool, which would lead to an 'El Niño-like' state. As some studies have shown, rainfall in northern Amazon is sensitive to the presence of circulation anomalies associated with strong El Niño or La Niña events [Marengo, 1992]. These anomalies are typified by lower than average rainfall and drought during El Niño. Marengo [2005] found that El Niño-related circulation and rainfall anomalies influence variability in the hydrometeorology of the northern Amazon region, while the southern region seems to be less affected by the remote tropical Pacific SST forcing.

These studies suggest the importance of moisture transport from adjacent oceans to the Amazon basin in determining seasonal and interannual variability of rainfall over this tropical forest. In order to identify if moisture transport from oceans could have been affecting cloudiness over the Amazon basin during the last decades, trends in vertical velocity (omega) over both land and oceans are analyzed. Results are linked with changes in SST and cloudiness over Amazon forests.

The upper panel of Figure 7.1 shows the seasonal trends in omega at 700 hPa from ERA-40 during 1984-2002 for DJF and MAM. Since omega at 700 hPa is negative over the Amazon basin during DJF and MAM (wet seasons are characterized by strong upward motion due to strong convective activity) negative (positive) trends over this region indicate enhanced (suppressed) upward motion. This suggests suppressed convection over the southern Amazon and enhanced upward motion over the northeastern Amazon, especially during MAM, which is consistent with the increase in high-level and decrease in mid-level clouds during this season observed in Figure 4.3. Decreasing trend in upward motion over the southern Amazon is also observed for JJA and SON.

Notice the north-south dipole over the equatorial Atlantic, which is stronger during MAM observed in Figure 7.1 (upper panel). To explain the consequences of this equatorial dipole on local vertical circulation, Figure 7.2 shows the seasonal mean omega vertical profile zonally averaged between 40°W and 20°W, which corresponds to the longitudes where the equatorial dipole is observed. Vertical profiles are showed from 20°S to 10°N. The region between the equator and 5°N, where negative trends in omega at 700 hPa are observed (Figure 7.1), is characterized by strong upward motion during DJF and MAM, while the one

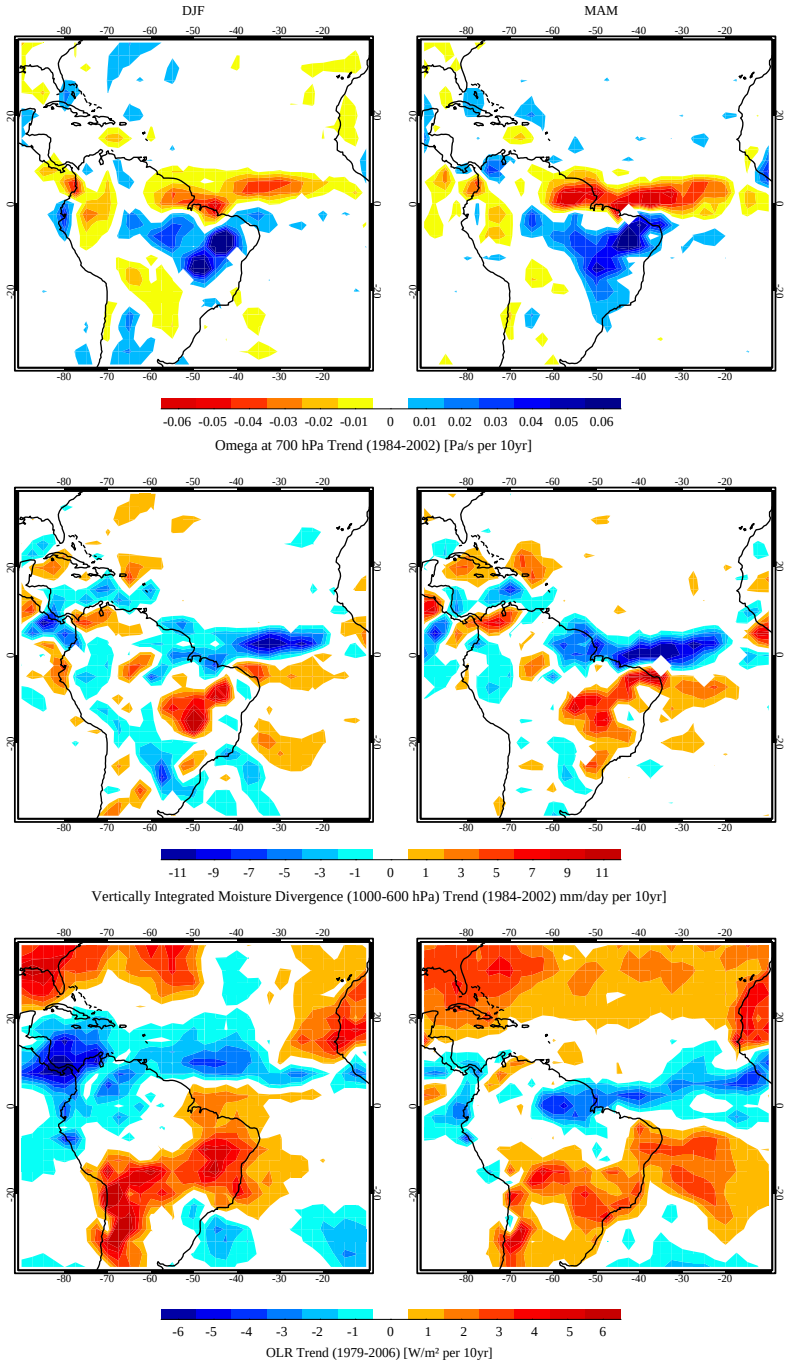

Figure 7.1: DJF and MAM trends in vertical velocity (omega) at 700 hPa from ERA-40, vertically integrated moisture divergence (1000-600 hPa), and OLR from NOAA during 1984-2002 (1979-2006 for OLR) over the Tropical Americas and Atlantic Ocean. Trends are significant at 95% according to the Mann-Kendall test with Sen's statistic [Sen, 1968].

located south of the equator is a subsidence region (positive omega) throughout the entire year. This indicates enhanced upward motion over the north equatorial Atlantic and stronger subsidence over the south equatorial Atlantic during the last decades. Mean profiles for JJA and SON show a northward expansion of the subsidence region and northward displacement of the convective region over the equatorial Atlantic during these seasons. This is consistent with the furthest northward migration of the Atlantic ITCZ during boreal summer (JJA).

Middle and lower panels of Figure 7.1 show DJF and MAM trends for vertically integrated moisture divergence (VIMD) obtained from ERA-40 data and OLR from NOAA, respectively. Moisture divergence is integrated between 1000 and 600 hPa. Trends for both variables show the same pattern than trends for omega at 700 hPa. Enhanced upward motion over the north equatorial Atlantic and northeastern Amazon is associated with decreased moisture divergence (increased convergence) and decreased OLR due to increased convective clouds. The opposite occurs over the south equatorial Atlantic and southern Amazon where trends indicate suppressed convective activity during the recent years. These results agree with positive trends in high-level clouds observed previously in Figure 6. The change in moisture transport is likely to cause changes in cloudiness over the Amazon basin.

OLR trends show the stronger positive trends over the Amazon basin during SON (not shown here) in agreement with the stronger negative trends observed in ISCCP total cloud cover during this season (Figure 4.1), showing consistency between both databases and, hence reliability in ISCCP cloud trends over the Amazon basin.

Seasonal trends for SST are shown in Figure 7.3. It is remarkable the dipole over the

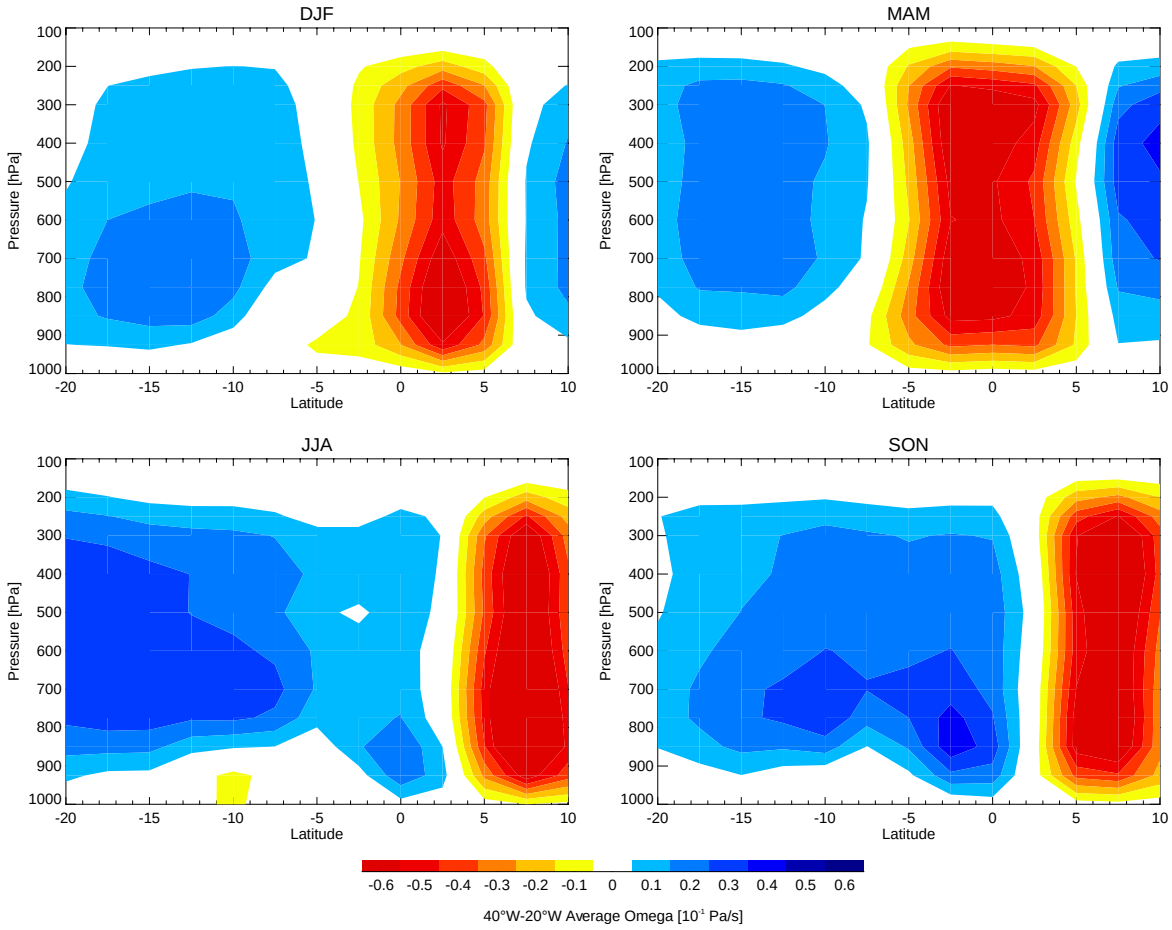

Figure 7.2: Seasonal mean vertical profile for zonally averaged omega over the western Atlantic (40°W and 20°W).

equatorial Atlantic, with positive trends to the north and negative to the south, suggesting a stronger SST gradient during 1984-2002. The existence of this SST gradient indicates a stronger Atlantic ITCZ during all the seasons, especially in DJF and MAM. The east Pacific also appears to have strong warming and the ITCZ appears to become stronger, especially during MAM and JJA.

To identify if SST is associated with local vertical motion and convective cloudiness changes over the Amazon basin, seasonal correlations between SST and domain average omega at 700 hPa are represented by colors in Figure 7.4. Correlations with domain average high-level clouds are shown by dashed (positive) and dotted (negative) contours. Because trends are removed before correlations are calculated, these correlations are associated to interannual variability more than to long term changes. Correlations for northern Amazon domain average omega at 700 hPa and high-level clouds indicate a strong association with SST over Eastern Pacific during DJF and JJA. Results suggest that increased SSTs over Eastern Pacific are associated with weaker upward motion and, for instance, with decreasing high-level clouds over northern Amazon during these seasons. This pattern is associated with ENSO, which typically reduces precipitation over northern Amazon during El Niño [Marengo, 1992]. Increasing North Atlantic SSTs are also correlated with suppressed upward motion over the northern Amazon during DJF. Decreasing SSTs over southern equatorial Atlantic is correlated with increase in subsidence over northern Amazon during JJA, and for instance, decrease in cloudiness during this season.

Correlations between SST over equatorial Pacific and domain averages over southern Amazon suggest a linkage with ENSO during MAM. Correlations in JJA show a different

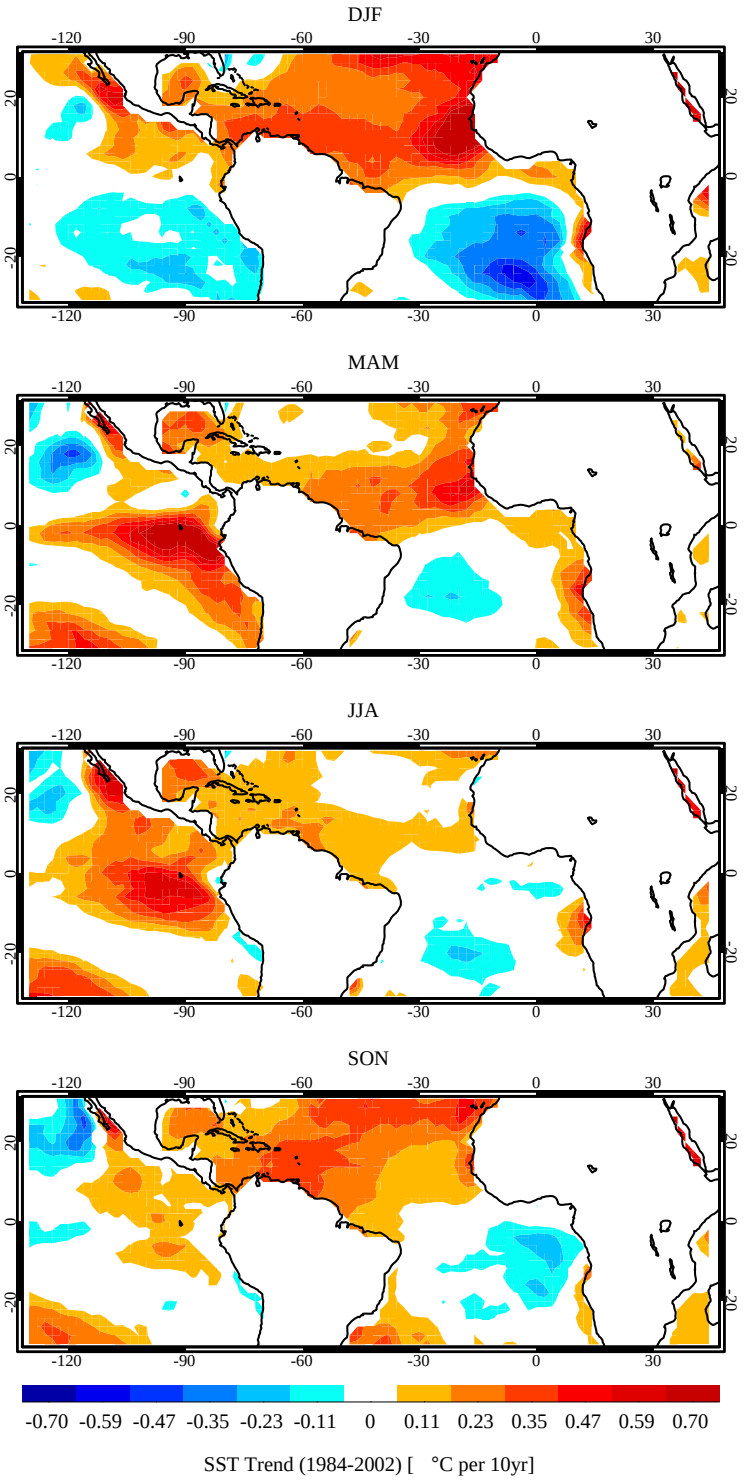

Figure 7.3: Seasonal trend in the Extended Reconstructed SST (ERSST) from NOAA-NCDC for the period 1984-2002. Trends are significant at 95% according to the Mann-Kendall test with Sen's statistic [Sen, 1968].

pattern. Increasing temperatures over north Atlantic and Caribbean Sea are correlated with decreasing upward motion and convective cloudiness over southern Amazon. Notice the large correlations with SST over the Indian Ocean during JJA. Positive trends in SST over Indian Ocean are associated with suppressed upward motion over the southern Amazon, reducing convective clouds during JJA, which corresponds to the dry season in southern Amazon and the Indian summer monsoon season.

Figure 7.5 shows seasonal correlations between Western Pacific / Caribbean Sea warm pool areas and ISCCP high cloud cover. Warm pools are selected as the areas with SSTs higher than 28°C and trends have been removed. Correlations indicate that Western Pacific warm pool area is negatively correlated with convective clouds over northern Amazon, especially during DJF, indicating decreasing high-level clouds with the larger areas of this warm pool. On the other hand, decreasing high-level clouds over southern Amazon appears to be correlated with the Caribbean Sea warm pool area during JJA. This suggests that at interannual scales, northern Amazon convective cloudiness is more associated to Pacific warm pool, while the southern Amazon is more associated with Caribbean Sea.

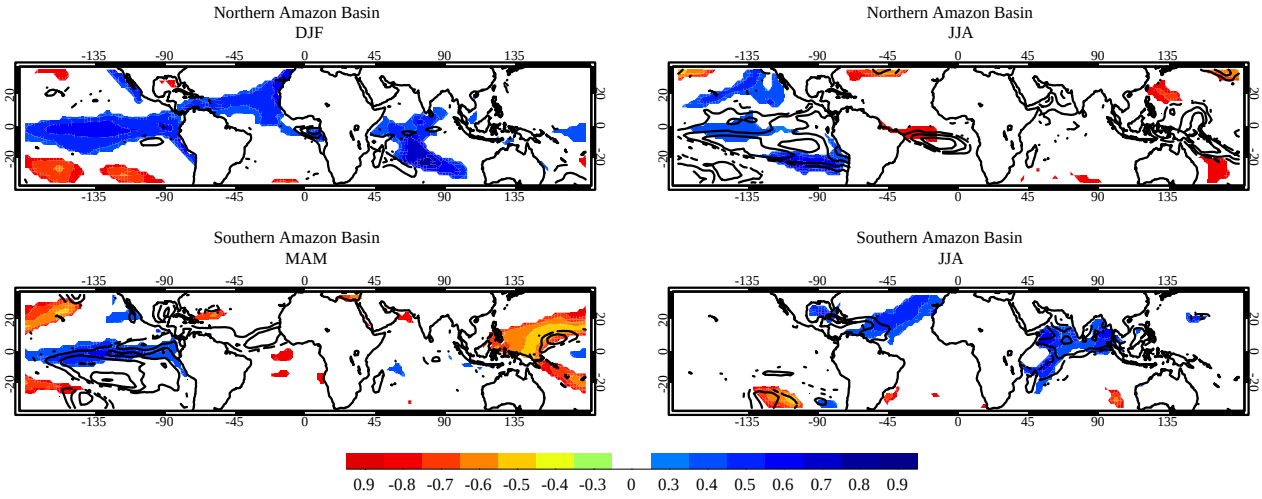

Figure 7.4: Seasonal correlations between SST and domain average omega at 700 hPa (colors). Contours represent correlations between SST and domain average high-level clouds. Dashed (dotted) lines represent positive (negative) correlations. Trends are removed before calculating the correlations. Correlations are significant at 95% level using a t-test.

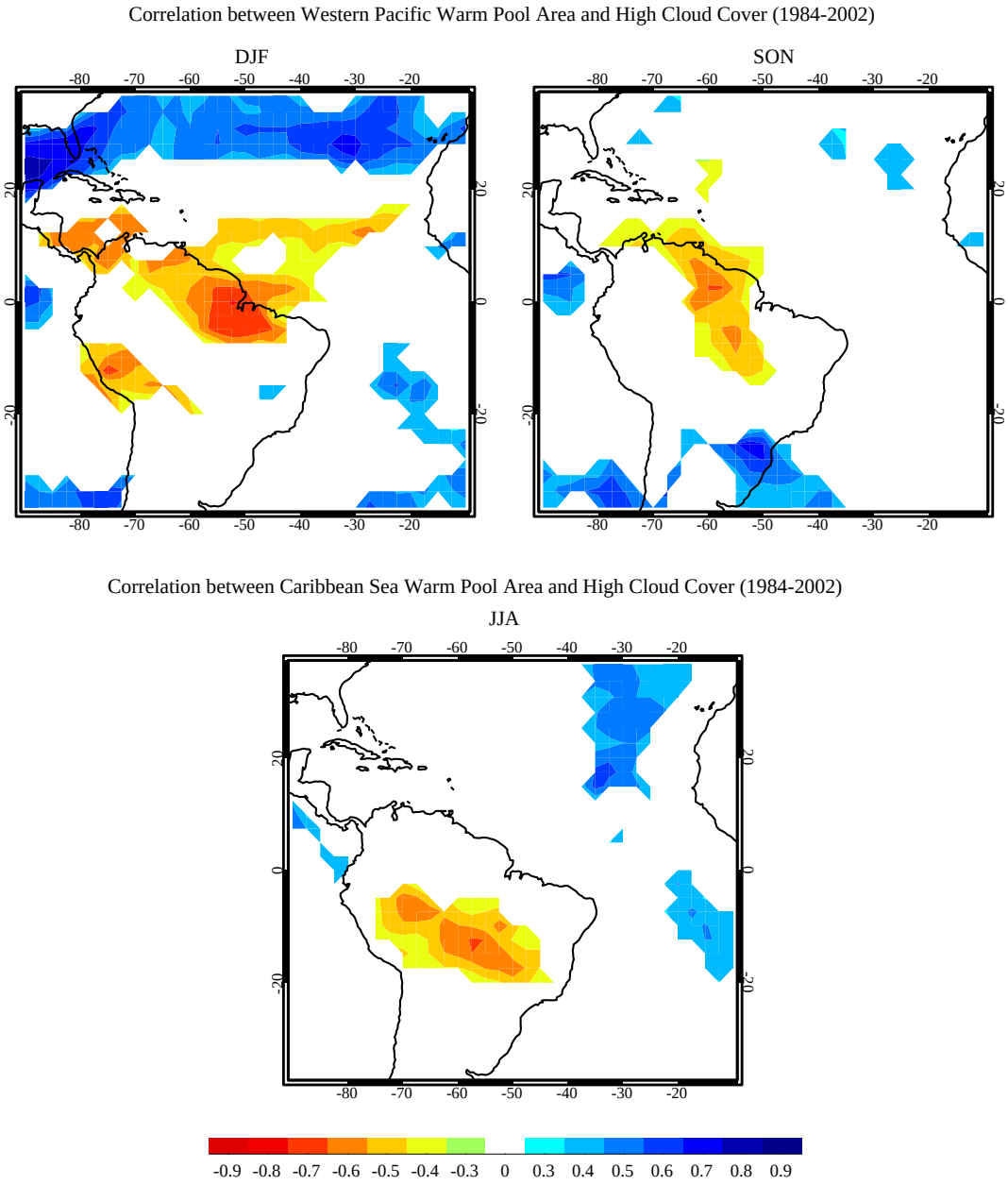

Figure 7.5: Seasonal correlations between Western Pacific / Caribbean Sea warm pool area and high-cloud cover over tropical America. Warm pools are selected as the areas with SST higher than 28°C. Trends are removed before calculating the correlations. Values over oceans are masked. Correlations are significant at 95% level using a t-test.

CHAPTER 8

CONCLUSIONS

This work has focused on changes in cloudiness observed during the past few decades (1984-2202) over Amazon and Congo tropical lands and their possible link to land surface and moisture transport changes.

Seasonal trends for shortwave (SW) downwelling radiation and different types of cloud cover from ISCCP were analyzed. A decrease in total and convective cloud cover over Amazon forests is observed, associated with an increase in downward solar radiation at surface, especially during SON (MAM) over the northern (southern) Amazon. A local increase in high-level (convective) clouds over northeastern Amazon is observed during MAM and shown to be consistent with changes in other variables. Reductions in total cloud cover over the Congo region are clear during MAM a SON, which correspond to the wet seasons in this forest. It is shown that the observed trends in cloudiness are not biased by changes in azimuth satellite angle detected in ISCCP satellites and, for instance the trend in downward solar radiation is not affected by changes in surface albedo.

To identify if changes in cloudiness are consistent with changes at land surface, station data given by Dai [2006] were used. Results indicate rising temperatures over both forests during all the seasons, stronger dry season over the Amazon forest, a drier transition season over the southern Amazon, and decreasing trend in relative and specific humidity over the

Congo basin during all the seasons. These findings are consistent with the dryer conditions over both forests during the past decades observed by several authors.

Vertically integrated moisture flux balance between 1000 hPa and 600 hPa levels calculated from ERA40 reanalysis has also decreased over these forests. Drier conditions in the mid-low troposphere over both the Amazon and Congo forests are observed, especially during the dry and transition seasons in the Amazon basin, consistently with the decrease in surface specific humidity observed from surface station data. Increase in meridional moisture flux balance during MAM over the northern Amazon is observed, consistently with the increase in high clouds found over the region during this season.

Radiosonde data over southern Amazon provided by University of Wyoming show a decrease of buoyancy and lower specific humidity in the troposphere during all the seasons, except in JJA due to strong surface warming. Calculations for CAPE indicate an increasing thermodynamic stability and a more elevated Level of Free Convection (LFC). These results suggest the increase of downward surface solar radiation since 1984 is the result from a decrease of convective and total cloudiness over the Southern Amazon basin, due to an increase of LFC and atmospheric thermodynamic stability. Whether this increase of surface SW radiation may have contributed to the increasing in growth rate in the Amazon forests and whether the observed changes are part of natural climate variability or due to anthropogenic influences needs to be investigated.

Although the goal of this study was not to focus on the determination of the impacts of deforestation and land use change in cloudiness over tropical forests, trends for Normalized

Difference Vegetation Index (NDVI) were calculated. Decreasing trends in NDVI (related to land use change) are observed over central-western Brazil during JJA and southern Brazil during SON, but these regions are located outside the domain considered in this study. A continuous band of increasing trend over the Sahel region is observed, in agreement with the greening trend observed over this region since 1983. Not significant trends are observed over Congo basin. NDVI trends suggest that severe land use changes do not take place over the domains analyzed in this study. However, the effect of vegetation and land use changes in cloudiness over these tropical forests needs to be addressed.

To observe if moisture transport from oceans has affected cloudiness over the Amazon basin during the last decades, trends in omega, OLR, and vertically integrated moisture divergence (VIMD) over both land and oceans were analyzed and linked with changes in SST and cloudiness over Amazon forests. Results indicate a north-south dipole in trends for omega at 700 hPa, VIMD, and OLR over equatorial Atlantic during DJF and JJA, which implies enhanced upward (downward) motion over north (south) equatorial Atlantic and is associated with a stronger SST gradient (stronger ITCZ) over the Atlantic Ocean. Enhanced (suppressed) upward motion, associated with increase (decrease) in moisture convergence over northeast (southern) Amazon is observed, in consistency with high-level clouds trend. The change in moisture transport is likely to cause changes in cloudiness over the Amazon basin. NOAA OLR trends are consistent with ISCCP high-level cloud trends observed over Amazon basin showing agreement between both databases and, hence reliability in ISCCP cloud trends over the Amazon basin.

Correlations for northern Amazon domain average omega at 700 hPa and high-level

clouds indicate a strong association with SST over Eastern Pacific during DJF and JJA, suggesting that increased SSTs over Eastern Pacific are associated with weaker upward motion and, for instance, decrease in high-level clouds over northern Amazon during these seasons. Decreasing SSTs over southern equatorial Atlantic is correlated with increase in subsidence over northern Amazon during JJA, and for instance, decrease in cloudiness during the dry season.

Increasing temperatures over north Atlantic and Caribbean Sea are correlated with decreasing upward motion and convective cloudiness over southern Amazon. Increased SST over Indian Ocean is associated with suppressed upward motion over the southern Amazon, reducing convective clouds during JJA, which corresponds to the dry season in southern Amazon and the Indian summer monsoon season.

Finally, correlations between warm pool areas and high-cloud cover suggests that at interannual scales, northern Amazon convective cloudiness is more associated to Pacific warm pool, while the southern Amazon is more associated with Caribbean Sea. Results obtained here suggest that changes in cloudiness over the Amazon basin can be associated with changes in moisture transport and SSTs over adjacent oceans. The underlying mechanisms of these effects need to be investigated.

REFERENCES

Adler, R.F., G.J. Huffman, A. Chang, R. Ferraro, P. Xie, J. Janowiak, B. Rudolf, U. Schneider, S. Curtis, D. Bolvin, A. Gruber, J. Susskind, and P. Arkin, 2003: The Version 2 Global Precipitation Climatology Project (GPCP) Monthly Precipitation Analysis (1979-Present). *J. Hydrometeor.*, **4,** 1147-1167**.**

Balas, N., S. E. Nicholson, and D. Klotter, 2007: The relationship of rainfall variability in West Central Africa to sea-surface temperature fluctuations. *Int. J. Clim.*, **27** (10), 1335-1349.

Campbell, G. G., 2004: View angle dependence of cloudiness and the trend in ISCCP cloudiness. Paper presented at 13th Conference on Satellite Meteorology and Oceanography, Norfolk, VA, 20-23 Sept (Available at *http://ams.confex.com/ams/pdfpapers/79041.pdf*).

Chagnon, F. J. F. and R. L. Bras, 2005: Contemporary climate change in the Amazon. *Geophys. Res. Lett,* **32**, L13703, doi:10.1029/2005GL022722.

Chagnon, F. J. F., R. L. Bras, and J. Wang, 2004: Climatic shift in patterns of shallow clouds over the Amazon, *Geophys. Res. Lett*, **31**: L24212, doi:10.1029/2004GL021188.

Chu, P.S., Z.P. Yu, and S. Hastenrath, 1994: Detecting climate change concurrent with deforestation in the Amazon basin: Which way has it gone? *Bull. Amer. Meteor. Soc*, **75**, 579-583.

Dai, A, 2006: Recent climatology, variability, and trends in global surface humidity. *J. Climate*, **19**, 3589-3606.

Evan, A. T., A. K. Heidinger, and D. J. Vimont, 2007: Arguments against a physical long-term trend in global ISCCP cloud amounts. *Geophys. Res. Lett.*, **34**, L04701, doi:10.1029/2006GL028083.

Foley, J., G.P. Asner, M.H. Costa, M.T. Coe, R. DeFries, H.K. Gibbs, E.A. Howard, S. Olson, J. Patz, N. Ramankutty, and P. Snyder, 2007: Amazon revealed: forest degradation and the loss of ecosystem goods and services in the Amazon basin. *Front. Ecol. Environ.*, **5**, 25-32.

Fu, R., R. E. Dickinson, M. Chen, and H. Wang, 2001: How do tropical sea surface temperatures influence the seasonal distribution of precipitation in the equatorial Amazon?, *J. Climate*, **14**, 4003–4026.

Fu, R. and W. Li, 2004: The influence of land surface on transition from dry to wet season in Amazonia, *Theor. Appl. Climatol., special LBA edition*, **78**, 97-110, doi:10.1007/s00704-004-0046-7.

Greco, S., and Coauthors, 1990: Rainfall and surface kinematic conditions over central Amazonia during ABLE 2B. *J. Geophys.Res.,* **95,** 17001–17014.

Hoyos, C.D and P.J Webster, 2007: Variability and expansion of the tropical ocean warm pool. 2007 AGU Fall Meeting, San Francisco, December 10-14.

Huete, A., K. Didan, Y. Shimabukuro, P. Ratana, S. Saleska, L. Hutyra, W. Yang, R. Nemani, and R. Myneni: 2006. Amazon rainforests green-up wutg sunlight in dry season. *Geophys. Res. Lett.*, **33**, L06405, doi:10.1029/2005GL025583.

Li, W. and R. Fu, 2004: Transition of the large-scale atmospheric and land surface conditions from the dry to the wet season over Amazonia as diagnosed by the ECMWF Reanalysis, *J. Climate*, **17**, 2637-2651.

Li, W. and R. Fu, 2006: Influences of cold air intrusions on the wet season onset over Amazonia. *J. Climate*, **19,** 257-275.

Li, W., R. Fu., R. Negrón Juarez, and K. Fernandes, 2008: Observed change of the Standardized Precipitation Index, its potential cause and implications to future climate in Amazon region. Submitted to *Phil. Trans. Roy. Soc*., (in revision).

Liebmann B. and C.A. Smith, 1996: Description of a Complete (Interpolated) Outgoing Longwave Radiation Dataset. *Bull. Amer. Meteor. Soc.*, **77**, 1275-1277.

Malhi Y., and J. Grace, 2000: Tropical forests and atmospheric carbon dioxide. *Trends in Ecology and Evolution*, **15**, 332-337.

Malhi, Y., E. Pegoraro, A.D Nobre, M.G.P Pereira, J. Grace, A.D Culf, and R. Clement, 2002: Energy and water dynamics of a central Amazonian rain forest. *J. Geophys. Res.*, **107**, doi:10.1029/2001JD000623.

Malhi, Y and J. Wright, 2004: Spatial patterns and recent trends in the climate of tropical rainforest regions. *Phil. Trans. R. Soc. Lond.*, **359**, 311-329.

Marengo, J. A., 1992: Interannual variability of surface climate in the Amazon basin, *Int. J. Climatol.*, **12**, 853–863.

Marengo, J.A, 2004: Interdecadal variability and trends of rainfall across the Amazon basin. *Theor. Appl. Climatol.* ,**78**, 79–96.

Marengo, J.A, 2005: Characteristics and spatio-temporal variability of the Amazon River basin water budget. *Clim. Dynamics*, **24**, 11-22.

Marengo, J., U. Bhatt, and C. Cunningham, 2000: Decadal and multidecadal variability of climate in the Amazon basin. *Int. J. Clim,*.

Negri, A.J., R. Adler, L. Xu, and J. Surrat, 2004: The impact of Amazonian deforestation on dry season rainfall. J. Climate, **17**, 1306-1319.

Nemani, R., C.D. Keeling, H. Hashimoto, W. Jolly, S. Piper, C. Tucker, R. Myneni, and S. Running, 2003: Climate-driven increases in Global Terrestrial Net Primary Production from 1982 to 1999. *Science*, **300**, 1560-1563.

Nepstad, D., G. Carvalho, A.C. Barros, A. Alencar, J.P. Capobianco, J. Bishop, P. Moutinho, P. Lefebvre, U. Lopes Silva Jr., and E. Prins, 2001: Road paving, fire regime feedbacks, and the future of Amazon forests. *Forest Ecology and Management*, **154** (3), 395-407.

Norris, J.R., 2000a: What can cloud observations tell us about climate variability? *Space Sci. Rev.*, **94**, 375–380.

Norris, J.R, 2005a: Multidecadal changes in near-global cloud cover and estimated cloud cover radiative forcing. *J. Geophys. Res.,* **110,** D08206, doi:10.1029/2004JD005600.

Olsson, L., L. Eklundh, and J. Ardo, 2005: A recent greening of the Sahel - trends, patterns and potential causes. *J. Arid Environ.*, **63**, 556-566.

Phillips, O.L., Y. Malhi, N. Higuchi, W.F. Laurance, V.P. Nuñez, R.M. Vásquez, S.G. Laurance, L.V. Ferreira, M. Stern, S. Brown, and J. Grace, 1998: Changes in the carbon balance of tropical forest: evidence from long-term plots. *Science*, **282**, 439-442.

Rao G.V and Erdogan, S, 1989: The atmospheric heat source over the Bolivian plateau for a mean January. *Bound. Lay. Meteor.*, **46**, 13-33.

Reynolds, R. W., 1988: A real-time global sea surface temperature analysis. *J. Climate*, **1**, 75-86.

Rossow, W.B., and Schiffer, R.A., 1999: Advances in understanding clouds from ISCCP. *Bull. Amer. Meteor. Soc.*, **80**, 2261-2288.

Saleska, S.R, S.D. Miller, D.M. Matross, M.L. Goulden, S.C. Wofsy, H.R da Rocha, P.B. de Camargo, P. Crill, B.C. Daube, H.C. de Freitas, L. Hutyra, M. Keller, V. Kirchhoff, M. Menton, J. W. Munger, E. H Pyle, A. H. Rice, H. Silva: 2003. Carbon in Amazon forests: Unexpected seasonal fluxes and disturbance-induced losses. *Science*, **302**, 1554-1557.

Sen, P.K, 1968: Estimates of the regression coefficient based on Kendall's Tau. *Amer. Stat. Assoc. J.*, **63**, 1379-1389.

Shukla, J., Nobre, C., and Sellers, P, 1990: Amazon deforestation and climate change. *Science* **247**, 1322--1325.

Simmons, A. J. and J. K. Gibson, 2000: The ERA-40 project plan, ERA-40 Proj. Rep. Ser. 1, 62 pp., Eur. Cent. for Medium-Range Weather Forecasts, Reading, UK.

Wang, H., and R. Fu, 2002: Cross-equatorial flow and seasonal cycle of precipitation over South America. *J. Climate*, **15**, 1591-1608.

Warren, S.G., R.M. Eastman, and C.J. Hahn, 2007: A survey of changes in cloud cover and cloud types over land from surface observations, 1971-96. *J. Climate*, **20**, 717-738.

Wright, S.J and C. van Schaik, 1994: Light and the phenology of tropical trees. *Am. Nat.*, **143**, 192-199.

Zhang, G. J., 2002: Convective quasi-equilibrium in midlatitude continental environment and its effect on convective parameterization, *J. Geophys. Res.*, **107,** D14, 4220, doi:10.1029/2001JD001005.

Zhang, Y., R. Fu, H. B. Yu, R.E. Dickinson, 2008: Radiative effect of Biomass Burning Aerosols on the surface fluxes and clouds over the South America as determined by a regional climate model simulation. Submitted to *J. Geophys. Res.*, (accepted).